

DISASTER PREVENTION RESEARCH INSTITUTE

BULLETIN NO. 67

MARCH, 1964

INVESTIGATION ON THE ORIGIN  
MECHANISM OF EARTHQUAKES  
BY THE FOURIER ANALYSIS  
OF SEISMIC BODY WAVES  
(I)

BY

YOSHIMICHI KISHIMOTO

KYOTO UNIVERSITY, KYOTO, JAPAN

---

---

DISASTER PREVENTION RESEARCH INSTITUTE  
KYOTO UNIVERSITY  
BULLETIN

---

---

Bulletin No. 67

March, 1964

---

Investigation on the Origin Mechanism of Earthquakes  
by the Fourier Analysis of Seismic Body Waves (I)

By

Yoshimichi KISHIMOTO

## Investigation on the Origin Mechanism of Earthquakes by the Fourier Analysis of Seismic Body Waves (I)

By

Yoshimichi KISHIMOTO

### Abstract

The P-waves of forty earthquakes of various magnitudes, and focal depths in various regions, were subjected to Fourier analysis for the purpose of investigating the origin mechanism.

First, the changes of spectrum with the epicentral distance, the azimuth and the location of observation station, were examined. The spectrum of P wave does not seem to change greatly with epicentral distance, at least, in the range of distance from  $30^\circ$  to  $90^\circ$  and in the range of wave-period of 4 sec to 60 sec. The azimuthal change of spectrum of P wave seems to be serious in some large and shallow earthquakes.

It was still possible on the standpoint, particularly, of the phase spectrum, to classify most earthquakes into two groups. It was made clear that the earthquakes in one group have impulsive wave-form and their spectra of P wave are approximately expressed by the simple function,  $t^p e^{-1.2t}$ , where p is of the order of 1 to 4. When the magnitude is larger, the value of p increases. This group includes mostly the earthquakes deeper than a certain depth, say 40 km. P wave-form seems to become sharper with increase of the focal depth, if the earthquakes of the same order of magnitude are compared.

Another group includes mostly shallow earthquakes, P wave-form of which are oscillatory. P waves of these earthquakes are considered to consist of double shocks which are assumed to originate at the origin. Each of these double shocks seems to be of somewhat different spectral structure from that of the former group. These facts may suggest that there is some essential difference in the nature regarding the radiation mechanism of seismic body wave at the origin between the deep and shallow earthquakes.

## 1. Introduction.

Investigation of the origin mechanism of earthquakes has been successfully carried out by various means of research. The fault-plane solution method is one of the most effective means, giving many interesting characteristics about the origin mechanism [Hodgson, 1957, 1960; Honda, 1962]. On the other hand, many theoretical works regarding the radiation mechanism have been published, which enabled us to explain fairly well not only the so-called push-pull distribution of the initial P and S motion, but also the observed wave-forms in some cases. The seismic wave-form, however, is never simple. It is often noticed by seismologists that the wave-form of, say P wave, differs with the magnitude, focal depth, epicentral region and other factors. So it is believed that the detailed investigation of the spectral structure of seismic waves is an effective means as another approach to the problem of origin mechanism.

Nevertheless, such a kind of research on the spectral structure of, in particular, the body waves has not been fully carried out, mainly due to the following reasons; 1) inadequate characteristics of the seismograph for the wave-form analysis, 2) insufficient accuracy of the calibration of instruments and of the time keeping, and 3) the transient nature of the recorded motion, particularly in the portion of body waves.

Fortunately the establishment of many new seismic stations attached to the Dominion Observatory, Canada, has been rapidly carried out since 1961, and a fairly large amount of data has been accumulated up to the present time. The seismogram recorded by the Press-Ewing long-period seismograph at each station seems to be qualified enough to do such a kind of research by the spectral analysis. Under these circumstances, the spectral analysis of P wave was carried out in some detail in order to clarify the relation between the spectral structure of P wave and the radiation mechanism at the seismic origin. In the present article, (I), the results of analysis of P wave are presented, including some problems on the observational results, such as changes of spectrum with the epicentral distance, azimuth and location of station, and a classification of the observed spectrum. The consideration of the origin mechanism derived from these spectral analyses will be given in some detail in the succeeding article.

## 2. Method and data.

In the present research, the following procedure of the Fourier analysis was used. Let  $f(t)$  be a time function representing the ground motion at a given station.  $f(t)$  is expressed as follows;

$$f(t) = \frac{1}{\pi} \int_0^{\infty} S(\omega) \cos[\omega t + \phi(\omega)] d\omega \quad (1)$$

where the amplitude,  $S(\omega)$  and the phase angle,  $\phi(\omega)$  of each component wave are calculated as follows;

$$\left. \begin{aligned} S(\omega) &= \sqrt{(a(\omega))^2 + (b(\omega))^2} \\ \phi(\omega) &= \tan^{-1}(-b(\omega)/a(\omega)) \\ a(\omega) &= \int_{-\infty}^{\infty} f(t) \cos \omega t dt \\ b(\omega) &= \int_{-\infty}^{\infty} f(t) \sin \omega t dt \end{aligned} \right\} \quad (2)$$

As any wave motion is completely known by giving the amplitude and phase spectrum,  $S(\omega)$  and  $\phi(\omega)$  of each component, we shall take  $\phi(\omega)$  as well as  $S(\omega)$  into consideration in the following treatment.

As mentioned in the Introduction, the body wave portions on the seismogram are never stationary but transient, so that particular care is necessary to carry out the Fourier analysis of such a kind of record. For this reason, Kasahara [1957] used the method of the convolution integral, in which the original function,  $f(t)$ , is multiplied by a weight function,  $k(t)$ , and this modified function,  $f(t)k(t)$  is Fourier-analysed instead of the original one,  $f(t)$ . Following him, the following weight function was used in the present analysis,

$$k(t) = \exp[-c^2(t-t_0)^2/4] \quad (3)$$

where  $t_0$  corresponds to the arrival time of the initial motion. Assuming  $K(\omega)$  and  $F(\omega)$  as the Fourier transforms of  $k(t)$  and  $f(t)$  respectively,  $G(\omega)$  which is the Fourier transform of the multiplied function,  $f(t)k(t)$  is expressed by the convolution integral as follows; [Blackman and Tukey, 1958],

$$G(\omega_1) = \int_{-\infty}^{\infty} K(\omega_1 - \omega) F(\omega) d\omega \quad (4)$$

This equation means that the Fourier transform of the multiplied function  $f(t)k(t)$  is an average-over-frequency of the original spectrum  $F(\omega)$ . If  $K(\omega)$  is of a very sharp form with a maximum at zero frequency,  $G(\omega)$  will be very close to  $F(\omega)$ .

The shape of  $k(t)$  should be determined referring to the respective record analysed. Since the width of the P motion seems to be 30—45 sec for earthquakes of magnitude around 7, and 30 sec or shorter for smaller earthquakes on the seismogram of the Press-Ewing long-period seismograph, 30 sec from the initial motion was taken as the span of analysis for most earthquakes except some large earthquakes, for which 45 sec was adopted. 0.003 and 0.0015 were used as the values of  $c^2/4$  in the weight function for the former and the latter respectively. As the resultant spectrum should vary with the difference in the span and weight function, it seems necessary to know beforehand what degree of change of spectrum occurs by varying the span and weight function. In Fig. 1, four spectra corresponding to the different span and weight function are shown, calculated from the same record which is shown by the small figure. It is seen that the amplitude spectrum is smoother in the case of 0.003 than in 0.0015 and also

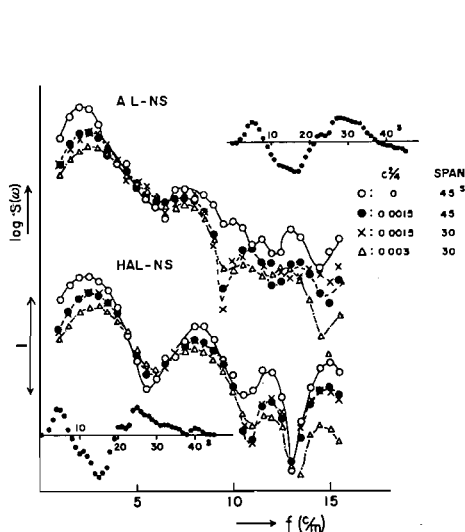


Fig. 1 The comparison of the method of analysis. Mexico, 1962 May 11 (No. 22). Hereafter the number in parentheses refers to Table 1.

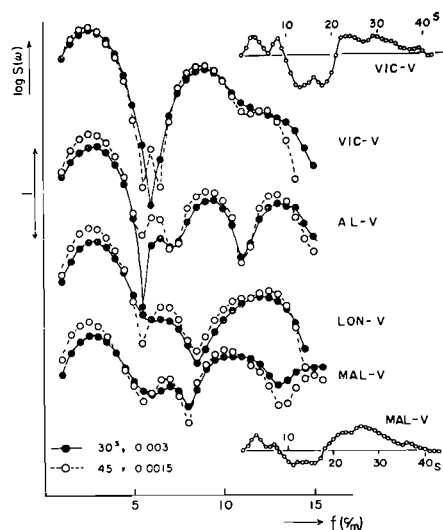


Fig. 2 The comparison of the method used. Mexico, 1962 May 19 (No. 33).

the case of 0.0015 gives a smoother curve than the case of no weight function. This result seems reasonable referring to the meaning of equation (4). There seems, however, to be no serious difference between them. The phase spectrum also does not show any large difference. Fig. 2 also shows the difference in two cases. It is seen in the figure that if the spectrum is of the flat shape the difference is small (London and Malaga), but the sharp trough in the spectrum differs in the two cases (Victoria and Mould Bay). The analysis with 0.003 gave only one sharp trough at about 5.5 c/m at Victoria and Mould Bay, while in the case of 0.0015 this trough was dissolved into two troughs which are close to each other. As will be mentioned in a later section, two troughs at Victoria and Mould Bay seem reasonable, and therefore the sharp trough in the spectrum should be carefully treated with.

The earthquakes analysed in the present study are mainly those which occurred in the period from the end of 1961 up to the end of 1962. Earthquakes were selected whose amplitude was large enough compared with the ground noise. Some old data in 1958, 1959 and 1960 were added, most of which were very deep earthquakes, because sufficient numbers of deep earthquakes were not available in this period from 1961 to 1962. The positions of epicenters and stations are shown in Fig. 3.

For the analysis of P wave, mainly the vertical component seismograph of the Press-Ewing long-period seismograph, an example of whose magnification curve is shown in Fig. 4, was used so far as it was available. Vari-

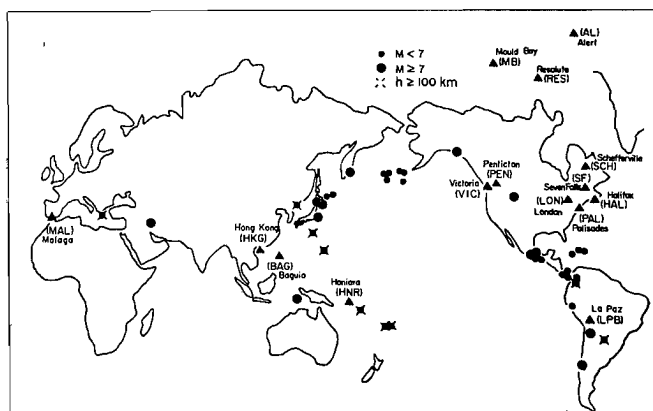


Fig. 3 Distributions of epicenters and observation stations.

Table I List of earthquakes used. The dates and origin times, epicenters and most focal depths are after USCGS. The focal depths with (\*) were estimated by the author. The magnitude is the mean of several estimations in each earthquake.

No.	Date	Origin time (U.T.)	Epicenter	Location	Focal depth km	Magnitude	Class. I	Class. II
1	1959 May 24	19 <sup>h</sup> 17 <sup>m</sup> 40 <sup>s</sup>	17 1/2N 97W	Mexico	100	6.8	A	A'
2	„ July 6	09 10 17	26 1/2S 61W	Argentina	600	6.6	„	„
3	1960 Oct. 8	05 53 01.1	40.0N 129.7E	Japan Sea	608	6.5	„	„
4	1961 May 23	02 45 16.0	36.4N 28.3E	Dodecanesese I.	49	6 1/4	„	„
5	1962 Jan. 8	01 00 24.2	18.5N 70.5W	Dominica	63	6.6	„	„
6	„ Mar. 7	11 01 00.4	19.3N 145.3E	Mariana I.	680	6.5	„	„
7	„ Apr. 18	19 14 37.2	10.0S 79.0W	Peru	55*	6.8	„	„
8	„ „ 20	05 58 55.3	20.6N 72.2W	Haiti	55*	6.5	„	„
9	„ „ 22	04 45 20.3	15.5N 93.1W	Mexico	69	5.4	„	„
10	„ „ 23	05 57 04.9	42.9N 143.4E	Japan	70*	7.1	„	„
11	„ May 22	08 06 38.7	12.3S 166.6E	Santa Cruz I.	151	6.3	„	„
12	„ Aug. 3	08 56 12.1	23.2S 67.5W	Chile-Argentina Border	71	7.0	„	„
13	„ „ 28	10 59 58.5	38.0N 23.1E	Greece	120	6.8	„	„
14	„ „ 31	17 02 43.4	51.3N 179.7W	Rat I.	26	6.4	„	B'
15	„ Sept. 1	03 46 05.0	51.3N 179.7W	„	42	6.1	„	„
16	„ „ 10	15 43 59.4	21.1S 179.2W	Fiji I.	650	6.5	„	A'
17	„ „ 18	00 29 05.2	7.5N 82.3W	Panama	33	6.9	„	„
18	„ Dec. 7	14 03 37.0	29.2N 139.2E	Bonin I.	411	6.9	„	„
19	„ „ 21	08 42 48.3	52.4N 168.5W	Fox I.	33	6.5	„	B'
20	„ „ 26	22 25 15.5	52.5N 168.8W	Komandorski I.	33	6.5	„	„
21	1961 Aug. 11	15 51 35.4	42.9N 145.1E	Japan	71	7.0	A?	„
22	1962 May 11	14 11 51.9	17.0N 99.7W	Mexico	25	7.1	A?	„
23	1958 July 10	06 15 —	58.6N 137.1W	Alaska	—	8	B	„
24	1959 May 4	07 15 42	52 1/2N 159 1/2E	Kamchatka	60	8	„	„
25	1961 Apr. 23	09 01 41.8	44.6N 150.2E	Kurile I.	44	6.4	„	„
26	„ Aug. 8	12 18 18.9	50.9N 170.7W	Fox I.	24	6.1	„	„
27	„ Dec. 20	13 25 34.4	4.6N 75.6W	Colombia	176	6.4	„	C'
28	1962 Feb. 14	06 36 01.3	38.1S 73.1W	Chile	44	7.4	„	B'
29	„ Mar. 12	11 40 12.8	8.1N 83.0W	Panama	58	6.6	„	C'
30	„ Apr. 12	00 52 47.0	38.2N 142.3E	Japan	68	7.0	„	B'
31	„ May 7	17 39 50.3	45.3N 146.7E	Kurile I.	25	6.5	„	„
32	„ „ 15	05 23 45.9	7.3S 128.2E	Banda Sea	34	7.3	„	„
33	„ „ 19	14 58 13.3	17.2N 99.5W	Mexico	20	7.1	„	„
34	„ „ 21	21 15 31.0	20.0S 177.5W	Fiji I.	379	6.9	„	C'
35	„ Sept. 1	19 20 38.5	35.6N 50.0E	Iran	21	7.3	„	B'
36	1959 Aug. 18	06 37 13	44.8N 111.1W	Hebgen Lake	—	7.1	?	?
37	1961 Dec. 30	00 39 24.1	52.3N 177.7E	Rat I.	32	6.8	?	?
38	1962 July 25	04 37 50.7	18.9N 81.1W	Jamaica	64	5.8	?	?
39	„ „ 26	08 14 41.8	7.5N 82.7W	Panama	21	6.9	?	?
40	„ „ 30	20 18 49.3	5.0N 76.3W	Colombia	45	6.8	?	?



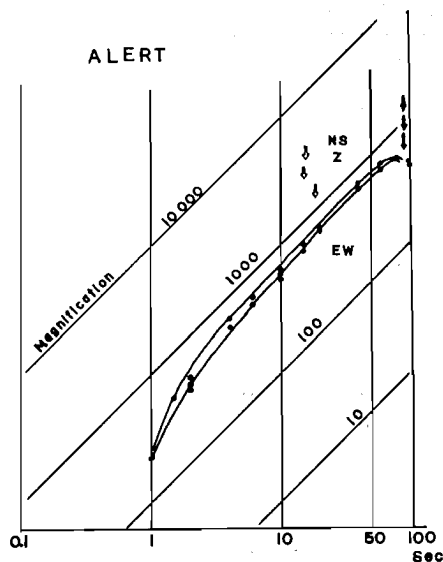


Fig. 4 Magnification curves of the Press-Ewing long-period seismograph at Alert.

ous data about the earthquakes analysed are listed in Table 1, in which the origin time, epicenter and focal depth (mostly) are after USCGS, and some focal depths were changed by the present author mainly from the time interval of P and pP. The magnitude is the mean of the values estimated at several observatories.

Some data obtained at the stations other than those in Canada were permitted for the author to analyse by the courtesies of respective stations. The name of station and the seismograph used are as follows:

Palisades, Honolulu and Hong Kong (Lamont Geological Observatory, Columbia University): Press-Ewing long-period.

Malaga, Baguio, Ponta Delgada, La Paz, Rabaul and Honiara (USCGS): World-wide Standard Seismograph.

Florissant (St. Louis University): Galitzin.

Lubbock (Texas Technological College): Press-Ewing long-period.

Cleveland (John Carroll University): Sprengnether.

### 3. Results.

#### (i) Amplitude and phase spectra.

The P waves of the earthquakes listed in Table 1 were Fourier-analysed.

The obtained amplitude and phase spectra are shown in Figs. 5 to 34, in which the amplitude spectrum is arranged in the order of epicentral distance. The abbreviation of the name of station should be referred to Fig. 3, and the numeral in the parentheses represents the epicentral distance in degree. Each amplitude spectrum is corrected by the magnification of seismograph and the phase spectrum is also corrected as to the instrumental phase shift. Since the instrumental phase shifts calculated for the respective stations of the Dominion Observatory do not differ greatly and are within the limit of the scatter of observation, the mean instrumental phase shift curve in which  $T_0=15$  sec,  $Tg=90$  sec,  $h_0=2.50$  and  $hg=0.65$ , was used for all the Press-Ewing long-period seismographs, except those at Resolute Bay and Ottawa. As for these two stations and other stations, the instrumental phase shift curves were calculated from their magnification curves.

The amplitude spectra in Figs. 5 to 34 are shown in logarithmic representation for the purpose of convenience of mutual comparison, and the abscissa shows the frequency per minute. In the graphs of phase spectrum, all observational points were so close at low frequencies that only the minimum and maximum points are plotted to avoid confusion.

**(ii) Changes of spectrum with the epicentral distance, azimuth and location of station.**

Needless to say, the spectral structure of any seismic wave is originally determined by the radiation mechanism at the origin, but it may undergo some changes during its propagation caused by, for instance, the reflection and refraction at the discontinuous surface, the absorption, the scatter and so on. It is an important problem to estimate and eliminate, if possible, these changes during the propagation in order to derive the radiation mechanism at the origin from the spectral structure of the observed seismic wave. Although it was not within the scope of the present study to thoroughly investigate this problem, some considerations will be given in this section.

*(a) Change of spectrum with the epicentral distance.*

The records of some earthquakes were available in fairly long distance-range. The records of the Haiti earthquake of Apr. 20, 1962 (No. 8 in Table 1, Figs. 8 and 10) were analysed in the distance-range from  $20^\circ$

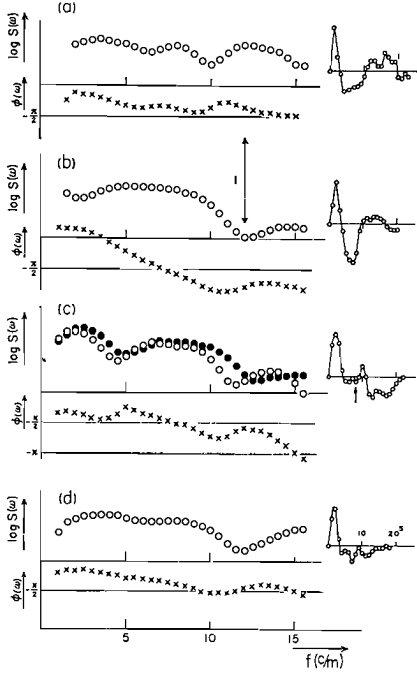


Fig. 5 Deep earthquakes (Group A).  
 (a) Argentina, 1959 July 6 (No. 2)  
 (b) Japan Sea, 1960 Oct. 8 (No. 3)  
 (c) Mariana Is., 1962 Mar. 7 (No. 6)  
 (d) Fiji, 1962 Sept. 10 (No. 16)

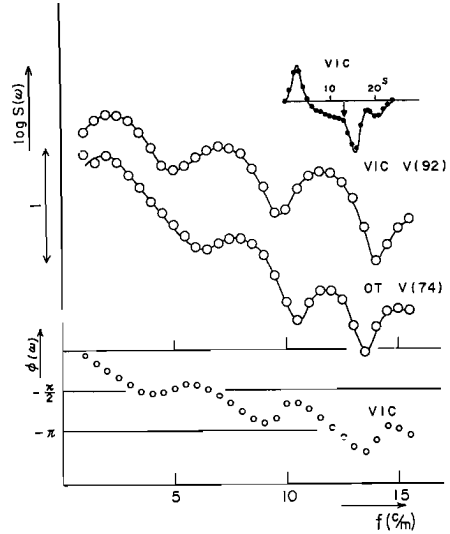


Fig. 6 Dodecanese, 1961 May 23 (No. 4)  
 (Group A)

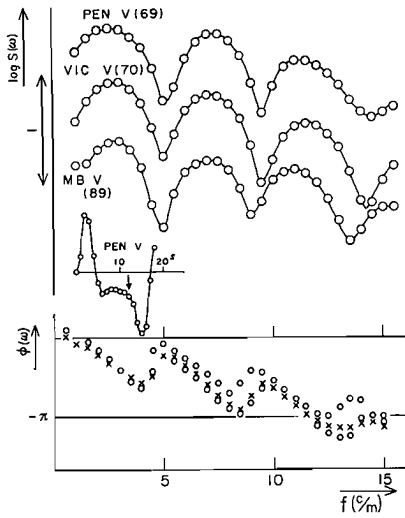


Fig. 7 Peru, 1962 Apr. 18 (No. 7)  
 (Group A)

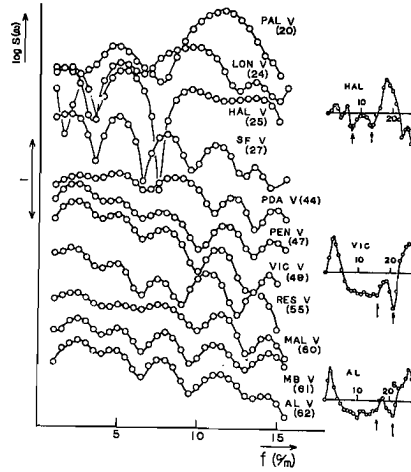


Fig. 8 Haiti, 1962 Apr. 20 (No. 8)  
 (Group A)

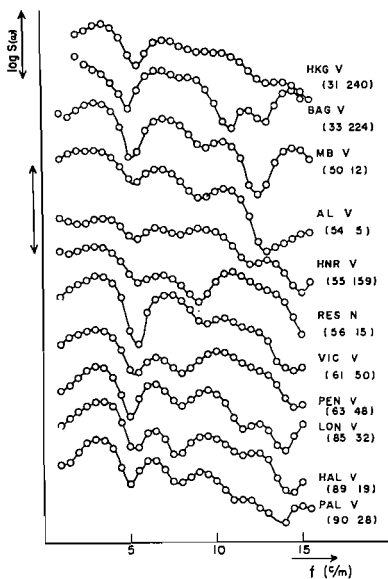
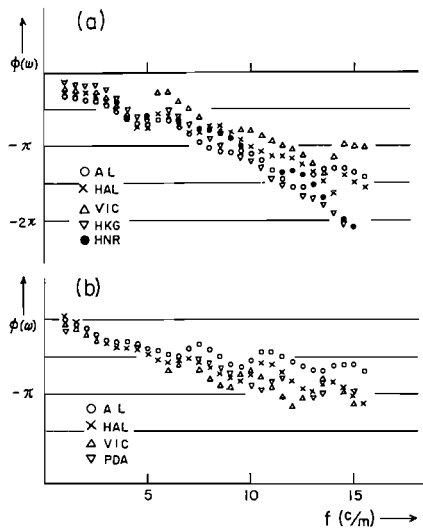


Fig. 9 Japan, 1962 Apr. 23 (No. 10) (Group A)



(a) Japan, Apr. 23, 1962  
M = 7.1, h = 70 km  
(b) Haiti, Apr. 20, 1962  
M = 6.8, h = 55 km

Fig. 10 (a) Japan, 1962 Apr. 23 (No. 10)  
(b) Haiti, 1962 Apr. 20 (No. 8)

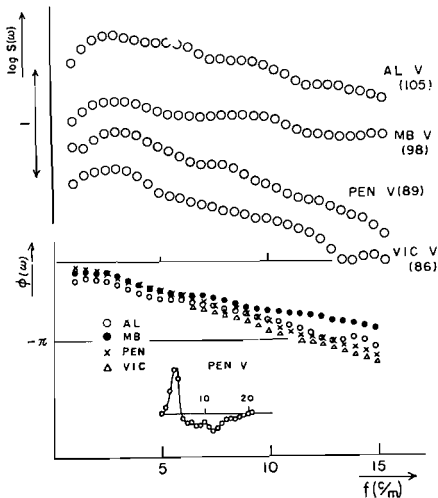


Fig. 11 Santa Cruz Is., 1962 May 22 (No. 11) (Group A)

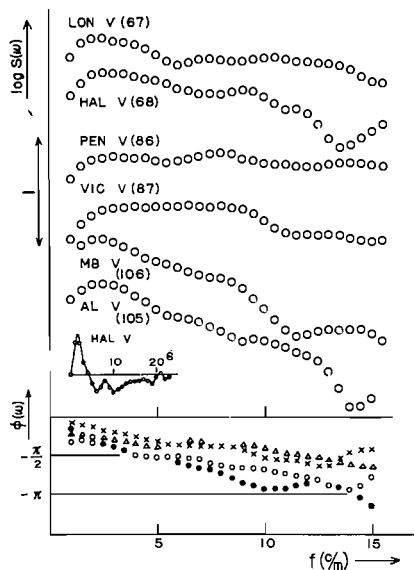


Fig. 12 Chile-Argentina border, 1962 Aug. 3 (No. 12) (Group A)

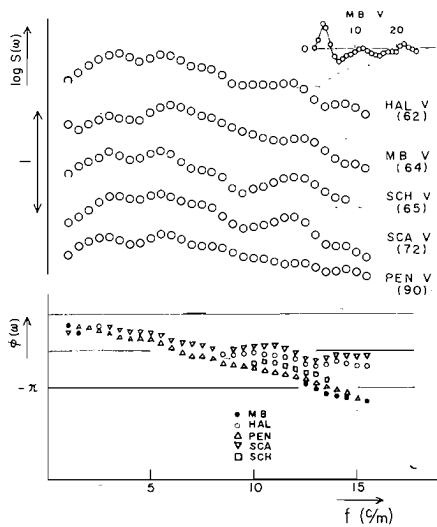


Fig. 13 Greece, 1962 Aug. 28 (No. 13)  
(Group A)

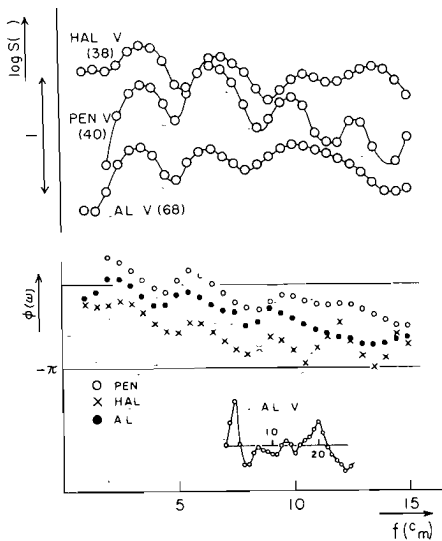


Fig. 14 Mexico, 1962 Apr. 22 (No. 9)  
(Group A)

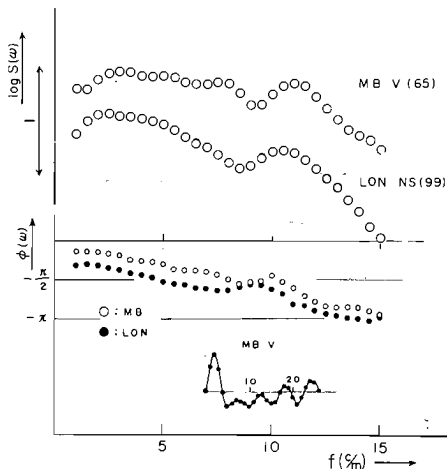
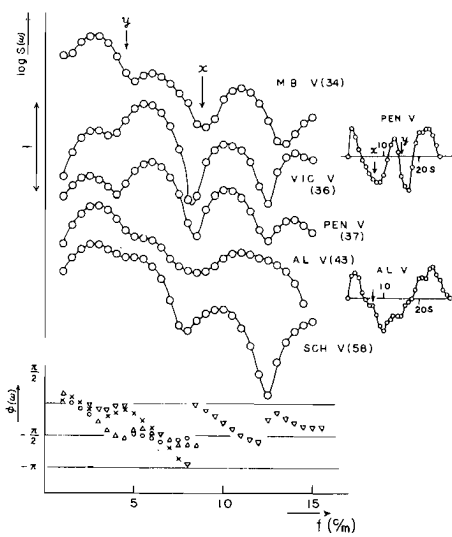


Fig. 15 Bonin Is., 1962 Dec. 7 (No. 18)  
(Group A)



Rat Is Aug. 31 1962  
M=6.4 h=26 km

Fig. 16 Rat Is., 1962 Aug. 31 (No. 14)  
(Group A)

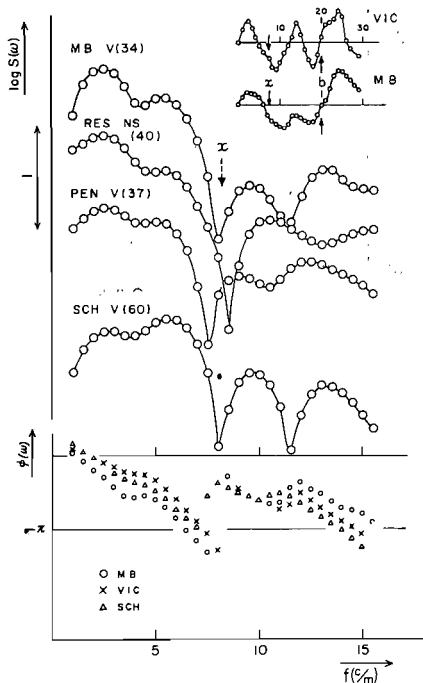


Fig. 17 Rat Is., 1962 Sept. 1 (No. 15) (Group A)

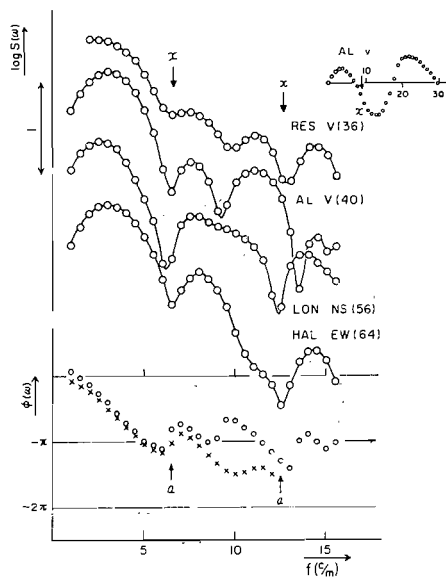


Fig. 18 Fox Is., 1962 Dec 21 (No. 19) (Group A)

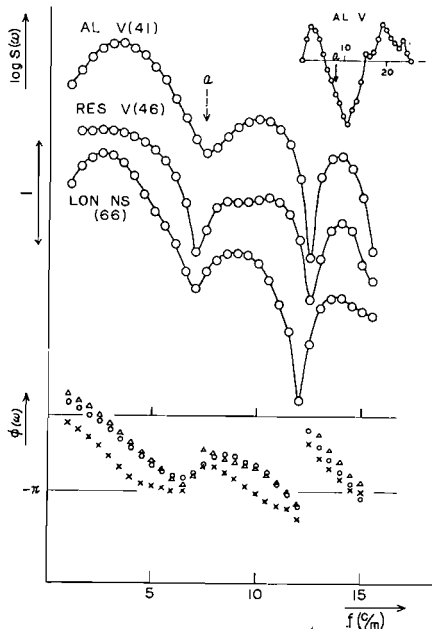


Fig. 19 Komandorski Is., 1962 Dec. 26 (No. 20) (Group A)

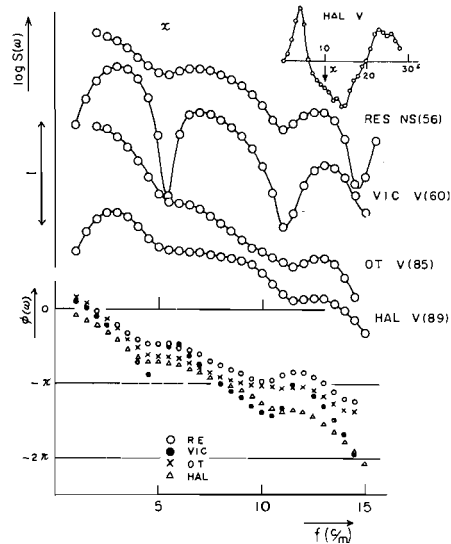


Fig. 20 Japan, 1961 Aug. 11 (No. 21) (Group A)

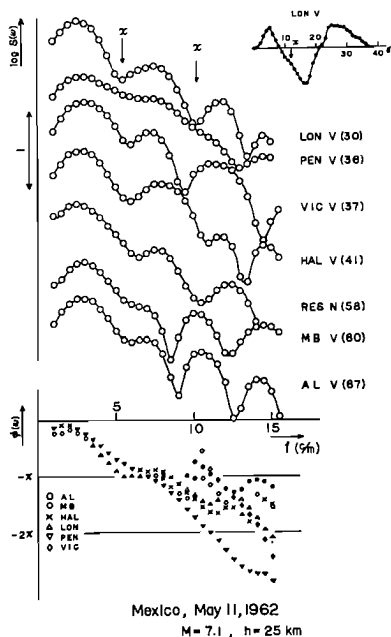


Fig. 21 Mexico, 1962 May 11 (No. 22) (Group A)

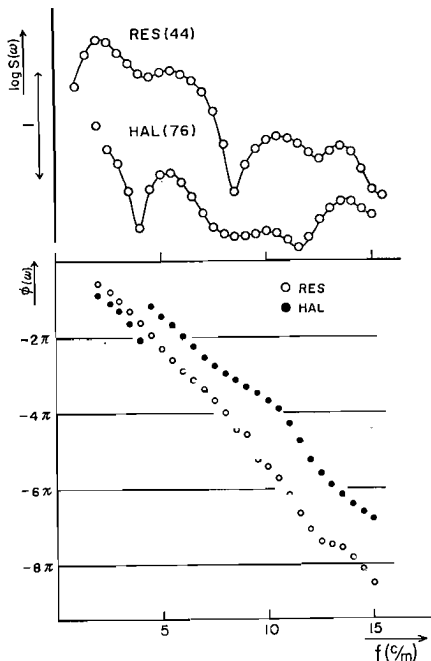


Fig. 22 Kamchatka, 1959 May 4 (No. 24) (Group B)

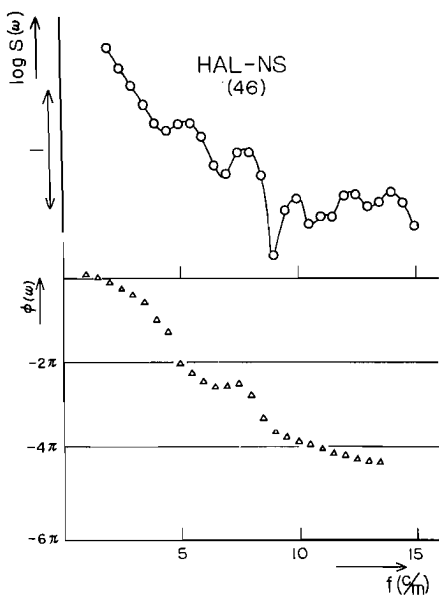


Fig. 23 Alaska, 1958 July 10 (No. 23) (Group B)

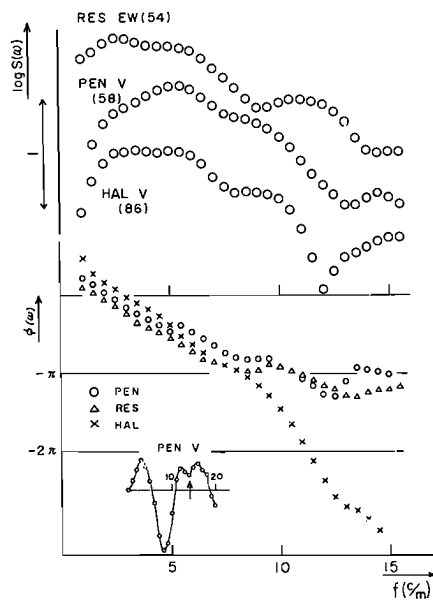


Fig. 24 Kurile Is., 1961 Apr. 23 (No. 25) (Group B)

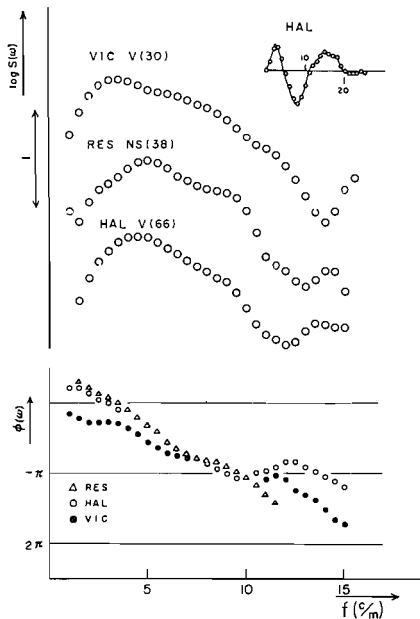


Fig. 25 Fox Is., 1961 Aug. 8 (No. 26) (Group B)

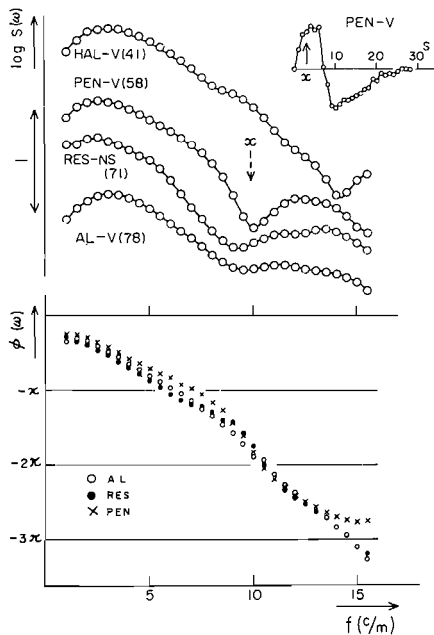
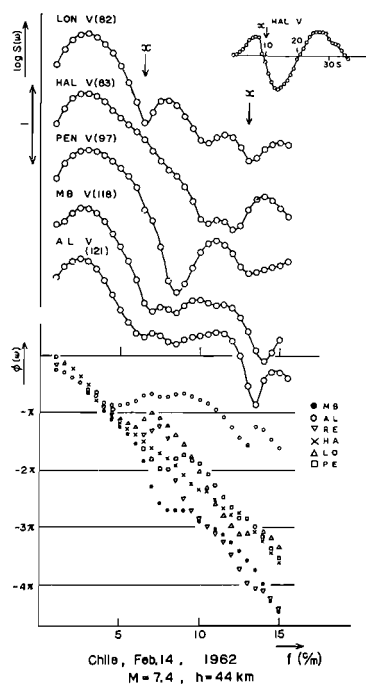


Fig. 26 Colombia, 1961 Dec. 20 (No. 27) (Group B)



Chile, Feb. 14, 1962  
M = 7.4, h = 44 km  
Fig. 27 Chile, 1962 Feb. 14 (No. 28) (Group B)

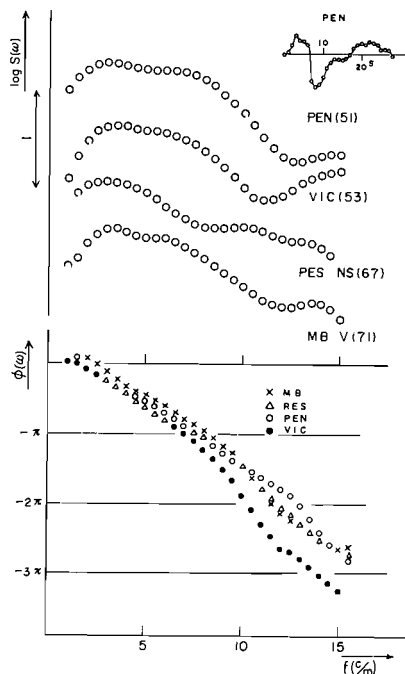


Fig. 28 Panama, 1962 Mar. 12 (No. 29) (Group B)



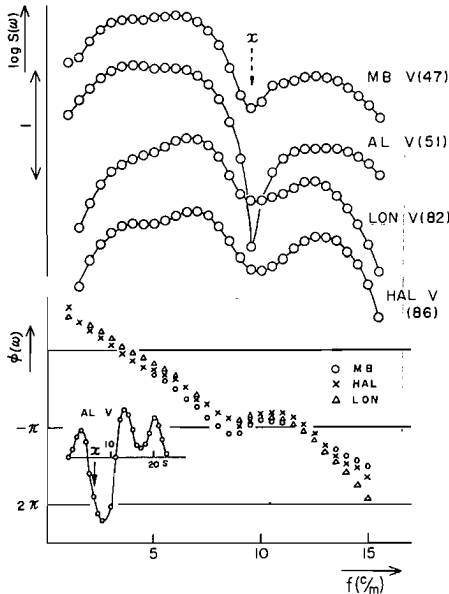


Fig. 29 Kurile Is., 1962 May 7 (No. 31) (Group B)

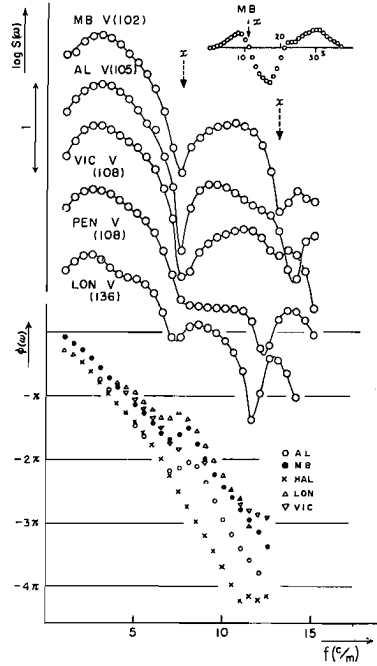


Fig. 30 Banda Sea, 1962 May 15 (No. 32) (Group B)

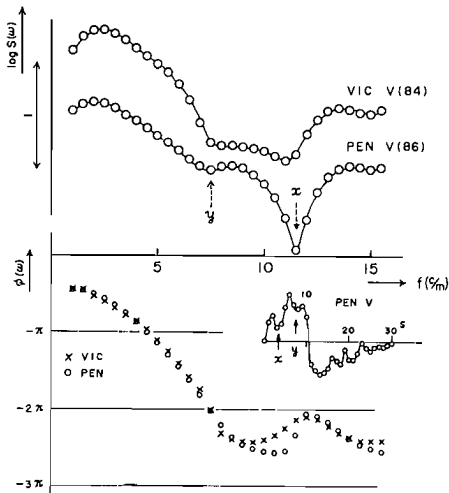


Fig. 31 Fiji, 1962 May 21 (No. 34) (Group B)

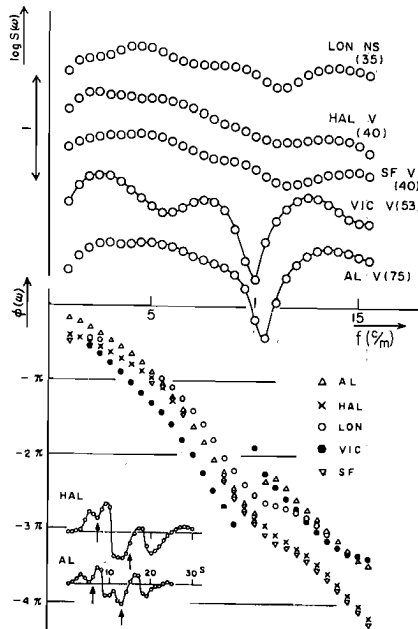
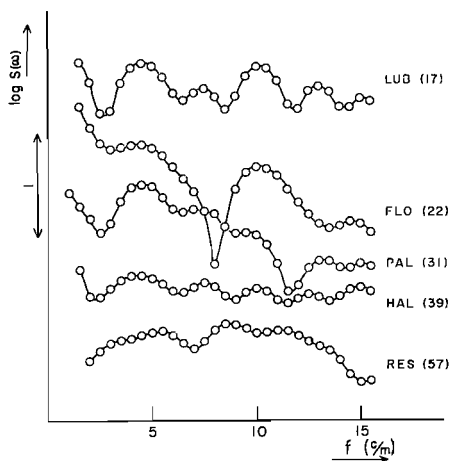


Fig. 32 Panama, 1962 July 26 (No. 39)



Mexico, May 24, 1959  
M = 6.9

Fig. 33 Mexico, 1959 May 24 (No. 1)  
(Group A)

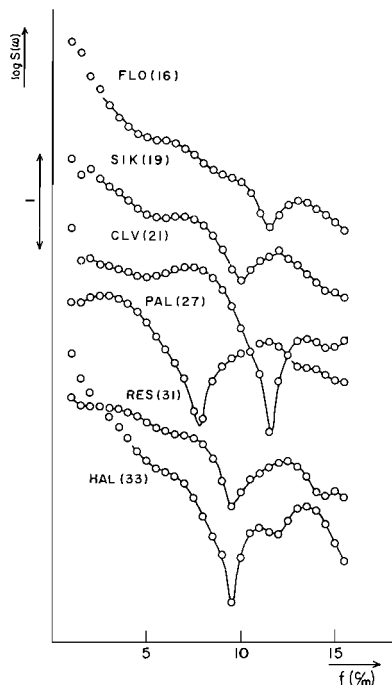


Fig. 34 Hebgen Lake, 1959 Aug. 1  
(No. 36)

to  $62^\circ$  which were all in the push region. As seen in both figures, the amplitude and phase spectra at all stations except three near stations, Palisades ( $20^\circ$ ), London ( $24^\circ$ ) and Halifax ( $25^\circ$ ), are very much alike with each other, and beyond, say,  $27^\circ$  (Seven Falls), we can not recognize any clear change of both spectra depending on the distance. (The phase spectra at three stations mentioned above are not given in Fig. 10 because of their irregular or unreasonable forms.)

The Japan earthquake of Apr. 23, 1962 (No. 10, Figs. 9 and 10) was analysed in the range from  $31^\circ$  up to  $90^\circ$ . In Fig 9, the first and second numerals in the parentheses are the epicentral distance in degree and the azimuth of station seen from the epicenter measured clockwise from the north in degree. In this earthquake, the records at Hong Kong, Baguio, Honiara and Palisades were analysed as well as the Canadian stations. It seems remarkable that all stations show the similar spectrum even for the fine structure, inspite of the differences in the epicentral distance and azimuth.

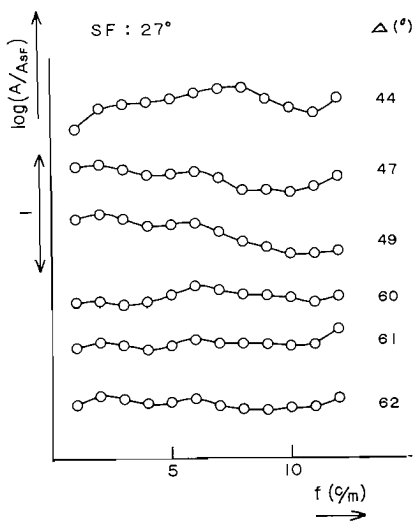


Fig. 35 Haiti earthquake of Apr. 20, 1962 (No. 8)

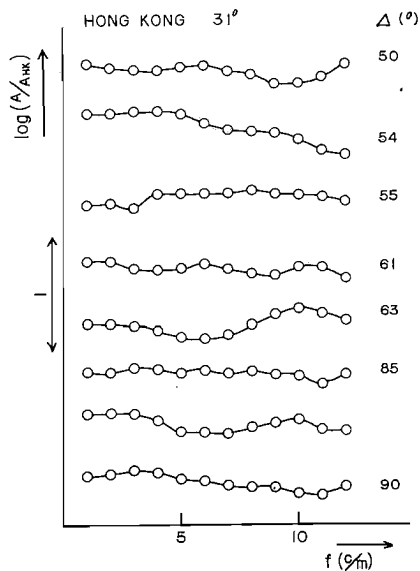


Fig. 36 Japan earthquake of Apr. 23, 1962 (No. 10)

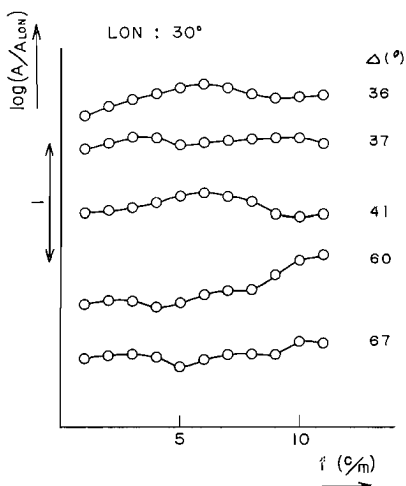


Fig. 37 Mexico earthquake of May 11, 1962 (No. 22)

In order to make clear this problem, the difference of spectrum between two stations was examined in some earthquakes. A periodic fluctuation of spectrum with frequency often observed on both amplitude and phase spectra is considered, as shown in the following section, to be caused by the superposition of a later phase of the same spectral structure. It seems reasonable, therefore, to consider an overlapped mean over frequency as the true spectrum of P wave. In Figs. 35, 36 and 37, the

amplitude ratio of two stations is shown, in which the nearest station with the epicentral distance close to  $30^\circ$  was taken as the standard. This amplitude ratio does not seem to change systematically depending on the epicentral distance. This fact is the same in the phase spectrum, too. Accordingly,

we may consider that the systematic changes of amplitude and phase spectra of P wave with epicentral distance are not serious, at least, in these ranges of distance and wave-period, say,  $30^\circ$ — $90^\circ$  and 4 sec—60 sec, respectively.

The problem is whether the spectrum observed in the above distance-range beyond  $30^\circ$  is basically the same as those radiated from the seismic source or not, and also how we may consider the peculiarity of the spectrum observed at short distances around  $20^\circ$ . As for the latter problem, it will be seen in a later section (iii) that this phenomenon is caused by the overlapping of some large later phase. Actually, as seen in Fig. 8, the seismograms at three stations are very complicated by overlapping of several large later phases, which may belong to various branches of travel-time curve of P wave near  $20^\circ$ .

The seismograms of two earthquakes, one in Mexico on May 24, 1959 (No. 1, Fig. 33) and another at Hebgen Lake on Aug. 19, 1959 (No. 36, Fig. 34), were available in the distance-range in which  $20^\circ$  is included. Although the seismograms at some stations were recorded by the short-period seismograph and many different types of seismograph are used, and therefore the mutual comparison is not so desirable, it seems that the same kind of peculiarity of spectrum near  $20^\circ$  is still observable, and moreover it does not seem that there is any great difference between two distance-ranges, namely one far beyond  $20^\circ$  and another shorter than  $20^\circ$ . Thus, we shall tentatively assume that the frequency-dependent distortion of spectrum is not so serious and that the spectra treated in the present study give the fundamental characteristics at the radiation from the source, if we eliminate the effect of overlapping of later phase in such a way as will be described in section (iii).

*(b) Change of spectrum with the azimuth.*

The azimuthal change of spectrum was already investigated by Kasahara [1960] in the case of the Alaska earthquake of Apr. 7, 1958. On the other hand, Ben-Menahem [1962] investigated the azimuthal change of spectrum of body wave when the seismic waves are assumed to be radiated from a moving source, and showed that Kasahara's results were explainable by his origin model. In the present analysis, four earthquakes were examined as to the azimuthal change of amplitude spectrum.

The Japan earthquake of Apr. 23, 1962 (No. 10, Figs. 9 and 10).

The amplitude and phase spectra are shown in Figs. 9 and 10, respectively. We can not recognize any systematic change depending on the azimuth, as already stated in the previous subsection.

The Iran earthquake of Sept. 1, 1962 (No. 35, Fig. 38).

Very clear P wave consisted of one and a half cycles of oscillation was recorded in this earthquake, as shown by the small figures on the left-hand side in Fig. 38. On the right-hand side of Fig. 38, the amplitude spectra at various stations are shown, arranged in order of the azimuth. It does not seem that there is any definite azimuthal change of spectrum. Malaga and Baguio are nearly in the opposite direction from the epicenter with each other, but the spectra as well as recorded wave-form at these two stations are quite similar.

The Japan earthquake of Apr. 12, 1962 (No. 30, Fig. 39).

As seen in Fig. 39, the seismograms in the pull region as well as the push region were analysed. Generally speaking, the wave-form and also amplitude spectrum of this earthquake are so complicated that it is difficult to give a reliable judgement, but the general form of the spectrum seems to be independent of the azimuth.

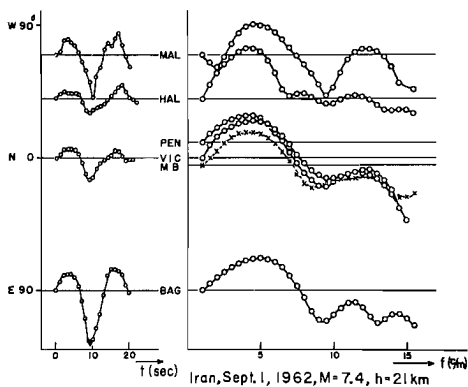


Fig. 38 Iran, 1962 Sept. 1 (No. 35)  
(Group B)

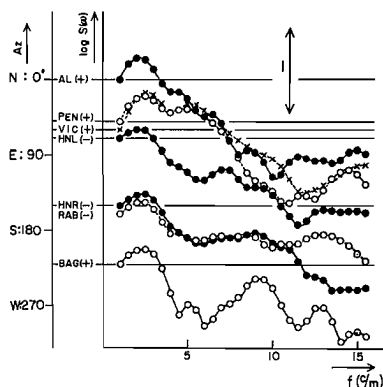


Fig. 39 Comparison of the amplitude spectrum in the Japan earthquake of Apr. 12, 1962 (No. 30)

The Mexico earthquake of May 19, 1962 (No. 33, Figs. 40 and 41).

The P waves observed at all stations consist of one and a half cycles of oscillation. In this example, the largest difference of azimuth was about  $180^\circ$  between Victoria and La Paz, but all stations were in the push

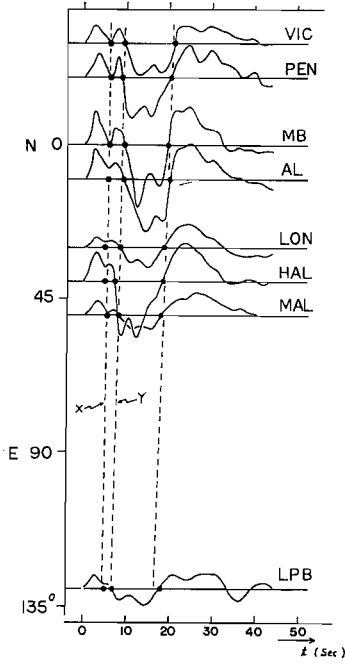


Fig. 40(a) Observed wave-forms of *P* in the Mexico earthquake of May 19, 1962 (No. 33)

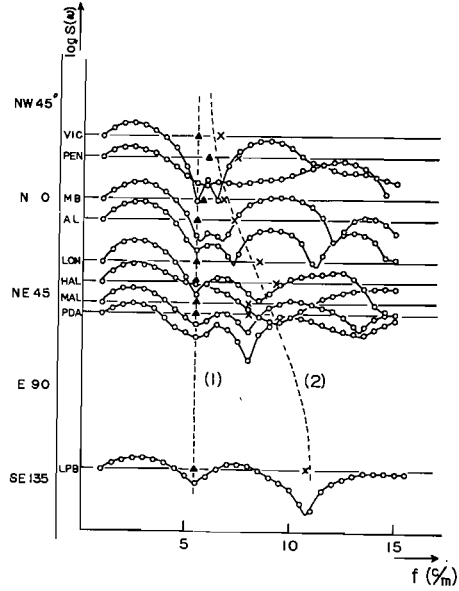


Fig. 40(b) Comparison of the amplitude spectrum in the Mexico earthquake of May 19, 1962

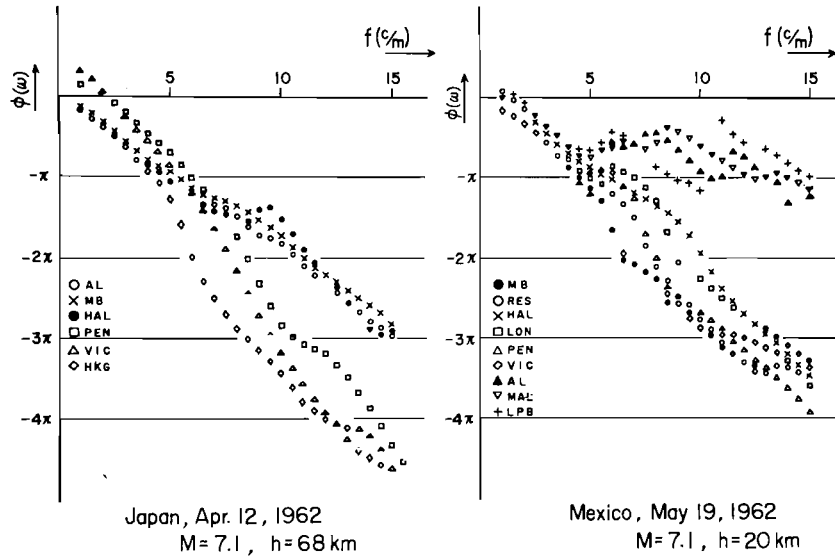


Fig. 41 Phase spectrum  
 (a) Japan, 1962 Apr. 12 (No. 30)      (b) Mexico, 1962 May 19 (No. 33)

region. In Figs. 40 (a) and (b), there seems to be clear dependence of the spectrum as well as the wave-form observed on the azimuth. In Fig. 40 (b), the first trough at about 5.5 c/m connected by a dotted line (1) is observed at all stations and exactly at the same position of frequency axis. As to the second trough, (2), the circumstances seem complicated, but it seems reasonable to interpret as follows: at Victoria, the second trough coincides with the first one and then, moving toward the higher frequency with the change of azimuth, it reaches about 11 c/m at La Paz which is situated at nearly the opposite direction from Victoria. This variation of spectrum does not depend on the epicentral distance, because the spectrum has quite a similar feature at London (30°), Ponta Delgada (67°) and Malaga (84°), inspite of their differences of distance. The observed wave-form seems also to vary azimuthally, as shown by the dotted lines in Fig. 40 (a).

If these identifications of two troughs are correct, several ways of explanation may be possible. If we assume both troughs (1) and (2) are caused by the later phases, one of them may be considered to have azimuthal characteristics. Comparing the amplitude spectrum with the observed wave-form, the following correspondence may be possible:

trough (1) . . . . phase  $x$ , the same sense as the initial motion,  $\tau=5$   
sec ( $\tau$  denotes the time interval from the initial motion).

trough (2) . . . . phase  $y$ , the opposite sense,  $\tau=10-6$  sec.

$\tau$  of the phase  $y$  is about 10 sec at Victoria and about 6 sec at La Paz. These values of  $\tau$  for  $x$  and  $y$  do not greatly contradict with the observed seismograms shown in Fig. 40 (a). As an example of explanation, we shall assume that this azimuthal change is caused by the movement of the source, and consider a simple model. In Fig. 40 (a), the points corresponding to each other on the respective seismograms shown by the letters  $x$  and  $y$  move toward the short period range, when we move from Victoria to La Paz. This fact seems to support the opinion that the moving source is plausible as the origin of this earthquake. Ben-Menahem [1962] worked out the azimuthal change of spectrum of the seismic body wave in the case of the strike slip fault. Following him, we shall assume a strike slip fault the length of which is  $b$ , extending in the direction from N40°W to S50°E. According to him, the frequency where the first trough of spectrum occurs by the effect of the movement of the source is given by

the following equation;

$$\frac{\omega b}{2V_a} \left( \frac{V_a}{V_f} - \cos \theta \right) = \pi$$

where

$\omega$ : angular frequency,  $b$ : fault length,  $V_f$ : rupture velocity,  $V_a$ : apparent P velocity for a given station,  $\theta$ : azimuth of the station measured from the direction in which the rupture advances. If we apply this equation for our simple model, it is possible to find out the suitable values of  $b$  and  $V_f$  by the trial and error method. In this case, if we put  $V_f = 3$  km/sec as the rupture velocity of the fault, 24 km is obtained as the fault length from observations at both stations, Victoria and La Paz. These values of rupture velocity and fault length do not seem so unreasonable, but more detailed investigation is needed for this problem. The dotted line (2) in Fig. 40 (b) was obtained by assuming the above model, showing the movement of the trough on the spectrum.

The results of these four examples tell us that the azimuthal change of spectrum seems fairly serious in some large and shallow earthquakes, and therefore particular care is needed in order to derive the origin mechanism from the spectral structure of seismic waves.

(c) *Change of spectrum depending on the location of the station.*

We can recognize in the results of some earthquakes the fact that the spectrum (amplitude spectrum in the main) shows some difference depending on the location of the observation station. Fig. 12 is a typical example of this phenomenon. Three pairs of stations, in each pair of which two stations are close to each other, namely, London and Halifax, Penticton and Victoria, and Alert and Mould Bay, seem to show respective features. The form of spectrum is very much alike at the two stations in each pair, while there is a systematic difference in comparison with any other pairs. The seismograms were available in many earthquakes at two pairs, Alert and Mould Bay, and Penticton and Victoria, so we shall examine the amplitude ratio of each Fourier component between these two pairs. The results in several earthquakes are shown in Fig. 42, in which the mean amplitude of two stations is taken as the representative value of each pair. In most cases, the amplitude ratio seems to change systematically with frequency. Although it is not clear from these results what the cause of this phenomenon is, we must take this fact into consideration, too.



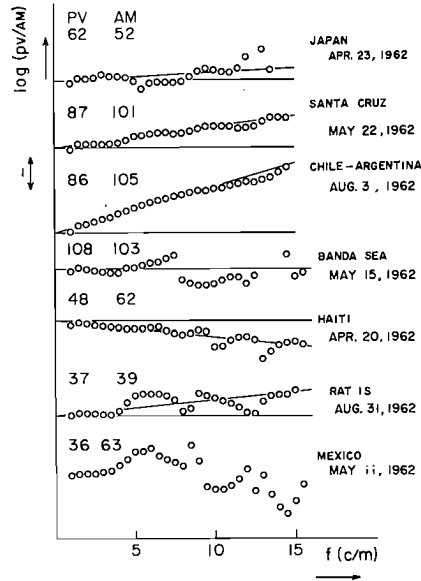


Fig. 42 Comparison of the observation stations.

In this section (ii), the changes of spectrum were examined as to various factors and it was found that such changes are, in some cases, not negligible, particularly regarding the azimuth. In spite of some changes above-mentioned, however, the fundamental feature of spectrum which is considered to originate at the seismic source is still kept in the respective earthquakes. Accordingly, the mean value of all stations will be tentatively assumed in the following to express the spectrum of the seismic wave radiating from the origin of the respective earthquakes.

**(iii) Effect of the later phase.**

Next it should be ascertained whether the obtained spectrum is exactly that of a seismic phase concerned or not. The distortion caused by multiplication of the weight function to the original seismogram and the change of spectrum with the epicentral distance and other factors were examined already in the earlier sections. Another serious distortion of the spectrum will be brought about by the overlapping of the later phase.

According to Kasahara [1957], the spectrum of a certain seismic phase overlapped by a later phase which has the same spectral structure is expressed as follows: let  $S(t)$  and  $S(t-\tau)$  be the wave-motions of the original

and overlapping phases respectively, and let  $S_0(\omega)$  and  $\phi_0(\omega)$  be the amplitude and phase spectra of the original phase. Then the spectrum of the overlapped wave is expressed as,

$$S_0(\omega) \cdot (1 + \alpha e^{-i\omega\tau}) e^{i\phi_0(\omega)}. \quad (5)$$

In this expression, the effect of overlapping is as follows:

$$\left. \begin{aligned} (1 + \alpha e^{-i\omega\tau}) &= \sqrt{(1 + \alpha \cos \omega\tau)^2 + \sin^2 \omega\tau} \cdot e^{i\phi_L(\omega)} \\ &\equiv L(\omega) e^{i\phi_L(\omega)} \\ \phi_L(\omega) &= \tan^{-1}(-\sin \omega\tau / 1 + \alpha \cos \omega\tau). \end{aligned} \right\} \quad (6)$$

The formula (5) becomes

$$L(\omega) \cdot S_0(\omega) \cdot e^{i(\phi_0(\omega) + \phi_L(\omega))}. \quad (7)$$

$L(\omega)$  and  $\phi_L(\omega)$  as the functions of  $\omega\tau$  are shown in Fig. 43.

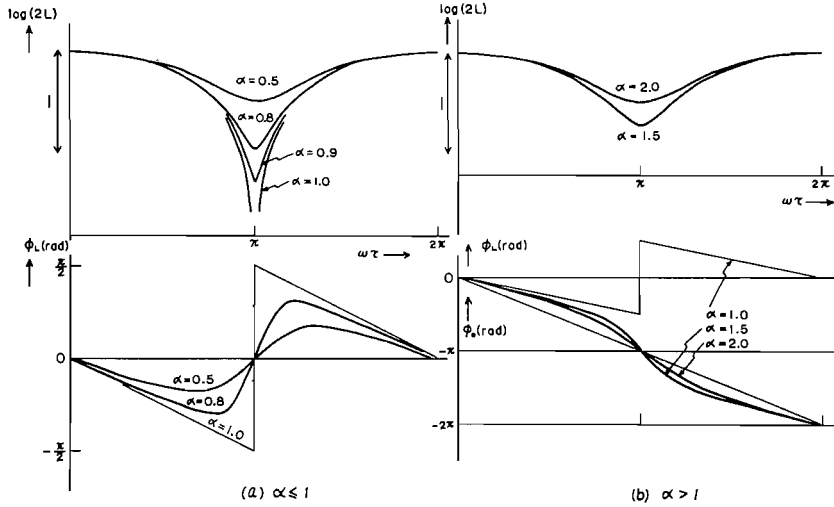


Fig. 43 Effect of latea phase.

For  $\alpha < 1$ , both  $L(\omega)$  and  $\phi_L(\omega)$  show nearly sinusoidal oscillations the period of which is  $2\pi$ . At  $\omega\tau = \pi$ ,  $L(\omega)$  has a minimum value, while  $\phi_L(\omega)$  becomes zero. When  $\alpha$  approaches to unity, the fluctuations of both graphs become larger, and for  $\alpha = 1$ ,  $L(\omega)$  becomes zero and  $\phi_L(\omega)$  jumps by  $\pi$  at  $\omega\tau = \pi$ . If  $\alpha$  increases over unity, the amplitude of  $L(\omega)$  begins to decrease again but  $\phi_L(\omega)$  changes its behaviour from the oscillation to a monotonous decrease with  $\omega\tau$  which amounts to  $-2\pi$  for one period of  $L(\omega)$ . (Fig.

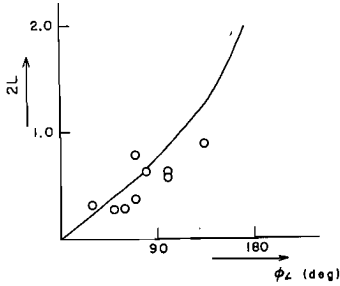


Fig. 44 Relation between both double amplitudes of fluctuations of the amplitude ( $2L$ ) and the phase ( $\phi_L$ ) caused by overlapping of the later phase.

43 (b)). The relation between the amplitudes of fluctuation of  $L(\omega)$  and  $\phi_L(\omega)$  is shown in Fig. 44 in the case of  $\alpha < 1$ . (Solid line in the figure).

There is the following relation between the time interval  $\tau$  and the period of change of  $L(\omega)$  and  $\phi_L(\omega)$ , this period being called  $\omega_0$ .

$$\omega_0 \tau = 2\pi \quad (8)$$

In the case of the later phase of the opposite direction of motion to the

initial phase, the graph in Fig. 43 should be moved by  $\pi$  in the negative direction of the abscissa. If we express the angular frequency where the first minimum occurs as  $\omega_1$ , there are the following relations;

$$\omega_1 \tau = \pi \quad \text{for the later phase of the same direction of motion,} \quad (9)$$

$$\omega_1 \tau = 2\pi \quad \text{for the later phase of the opposite direction of motion.} \quad (10)$$

Referring to these equations (9) and (10) and examining the observed spectra, it is possible to ascertain the incidence of the later phase, even if the wave motion is so complicated that it is hard to exactly identify the later phase on the seismogram.

Many complicated spectra shown in Figs. 5 to 34 are well explained as caused by the overlapping of the later phase in this way. It may be understood that many oscillatory spectra have exactly the same features as the theoretical ones in Fig. 43. The amounts of fluctuation of both amplitude and phase spectra were measured and plotted in Fig. 44 by the circle. Those points are all close to the theoretical line. Actually we can find a remarkable later phase on the seismogram with just the same time interval from the initial motion predicted from the spectrum. Thus we can safely consider an overlapped mean of the observed spectrum as that of the direct P wave.

(iv) **Classification of earthquakes by means of the phase spectrum.**

Amplitude spectra in Figs. 5 to 34 are rather complicated, having different forms from one earthquake to another, and in some cases from

station to station even for the same earthquake. On the other hand, the phase spectrum looks much simpler. The phase angle of each component wave is not uniquely determined but there is an ambiguity of  $2n\pi$ . It seems reasonable, however, to assume that the phase spectrum is fundamentally of as smooth a form as is the case in most simple functions which are usually assumed as the approximation of the wave-form of incidence. Therefore, in these figures, the value of  $n$  is selected so that the phase spectrum becomes as smooth as possible and that the phase angle has a value nearest to zero when it approaches to zero frequency. Most earthquakes have a phase spectrum which is approximately expressible by a linear decrease with frequency, although in some cases it is oscillatory and in other cases it has a rather large scatter of observation. The amount of this decrease, however, does not appear to be quite at random but it seems to have a value proper to each earthquake. We shall tentatively take the average of all stations as the representative of each earthquake. Fig. 45 shows the relation between the amount of negative inclination of the mean phase spectrum and the magnitude. In this figure, the ordinate shows the decrease of phase angle (rad.) per unit angular frequency (rad./sec).

It is recognized that the large proportion of plotted points clusters in two groups. The one group which clusters around the dotted line A is characterized by comparatively small amount of inclination (about 2 rad./rad./sec) which does not show clear correlation to the magnitude. (Strictly speaking, this group also has the correlation to the magnitude. It will be discussed in the next section.) It is interesting that almost all earthquakes of extremely deep focus belong to this group. Another group which is shown by the dotted line, B, has the feature that the inclination is much larger compared with the former group as seen in the figure, and it depends greatly on the magnitude. When the magnitude becomes large, the inclination increases rapidly. Most earthquakes in this group

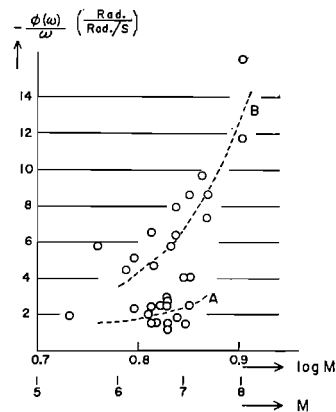


Fig. 45 Relation between the magnitude and the inclination of the phase spectrum.

are of the shallow focus. These two groups will hereafter for the purpose of simplicity be called group A and B for the former and the latter respectively. This classification is described in the 8th column of Table 1 which is headed by the classification I.

It can be seen that the wave-forms of P wave observed on the seismogram differ in these two groups, namely the P wave in group A is generally impulsive with the first sharp onset and large amplitude followed by the second back motion of small amplitude and long duration. On the other hand, the P wave in group B mainly is oscillatory with one and a half cycles of oscillation, the second and third swings sometimes being larger than the first one. These behaviours in both groups are clearly observable in the inserted wave motions in Figs. 5 to 34.

The amplitude spectrum in group A is generally simple. It has a maximum at a certain wave period (it is called  $T_0$  in the following) which may depend on the magnitude as pointed out by several authors and smoothly decreases on both sides of the maximum. The amplitude spectrum of group B also has the same maximum point, but it is generally complicated in the shorter period range. In Fig. 46, a relation between the magnitude and  $T_0$  is shown.

It is interesting that a large proportion of the data is classified into

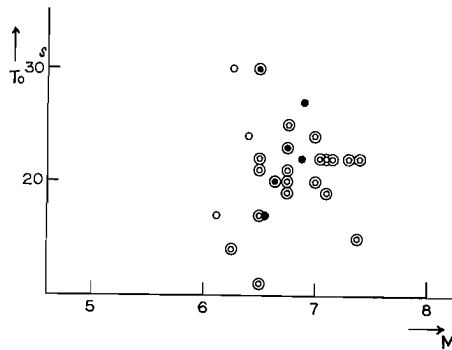


Fig. 46 Relation between the magnitude ( $M$ ) and the period ( $T_0$ ) where the spectral intensity is the maximum. White and black symbols represent the earthquakes shallower and deeper than 100 km, respectively. Double and single symbols represent the observation at 2 or more stations and 1 station, respectively.

a few groups from the viewpoint of spectral structure, inspite of the differences in the magnitude, the focal depth and epicentral region. This fact might suggest that the radiation mechanism is not so random, but that there exist a few patterns of radiation of seismic waves from the origin. In the following sections, we shall consider the characteristics of these groups in more detail.

(v) **Group A.**

This group is characterized by the small variation of the inclination of phase spectrum with the magnitude as stated in the foregoing section. But, the same tendency as in group B is still observable if we examine Fig. 45 more precisely. Fig. 47 (a) is a more detailed illustration of group A which shows the same relation as in Fig. 45, but it is drawn in an enlarged scale. In Fig. 47 (b), the focal depth is taken as the abscissa in place of the magnitude. In these figures, the ordinate represents the difference of phase angles at 1 and 15 c/m instead of the slope of the phase spectrum, because the spectrum is considerably curved in some earthquakes and it is difficult to determine the exact inclination. It is seen in Fig. 47 (a) that the phase spectrum also increases its inclination depending on the magnitude, although it is not so clear as in the case of group B. This

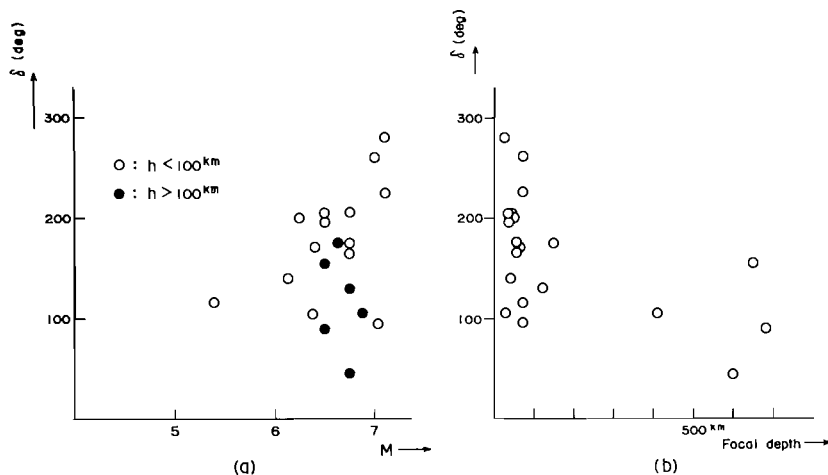


Fig. 47 (a) Relation between the magnitude ( $M$ ) and the inclination of the phase spectrum ( $\delta$ ).  
 (b) Relation between the focal depth and the inclination of the phase spectrum ( $\delta$ ).

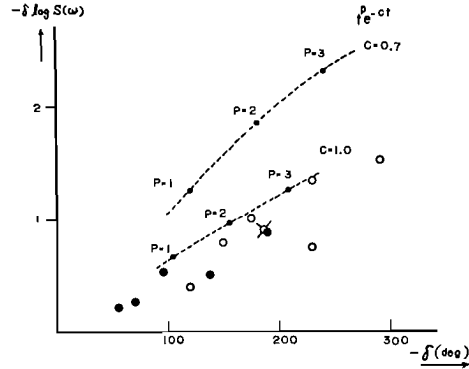


Fig. 48 Relation between the amplitude and phase spectra in the group A.

relation becomes clearer, if we consider only the earthquakes represented by the open circle which is shallower than 100 km. It is interesting to note that the earthquakes shown by the solid circle deeper than 100 km are situated generally in the lower portion of the figure compared with the shallower shocks.

The amplitude spectrum in this group is considered to be relatively simpler than that of group B. The inclination of the amplitude spectrum in the shorter period-range from the maximum point seems approximately linear decrease with frequency. The gradient of this linear decrease seems to be related systematically with the behaviour of the phase spectrum. Namely, the smaller the variation of phase spectrum with frequency is, the smaller the inclination of amplitude spectrum becomes, too. This relation is clearly seen in Fig. 48, in which the ordinate shows the difference of logarithms of amplitude at the maximum point and 15 c/m, and the abscissa is the same as in Fig. 47. It is possible to find out a simple function which approximately represents this observational relationship between the amplitude and phase spectra. The function  $t^p e^{-ct}$ , for instance, is a fairly good approximation, if the suitable values of  $p$  and  $c$  are selected. As shown in Fig. 48, the value of  $c$  is estimated as about 1.2, while  $p$  is of the order from 1 to 4 which may change depending on the magnitude. As seen in Fig. 47 (a), the phase difference between 1 and 15 c/m ( $\delta$  in the figure) is estimated as follows;

$$\begin{aligned} \delta &= 200^\circ \text{ or more for } M=7, \\ \delta &= 150^\circ \text{ or less for } M=6, \\ \delta &= 100^\circ \text{ or less for } M=5. \end{aligned}$$

Thus referring to Fig. 48, the approximate value of  $p$  is as follows;

$$\begin{aligned} &\text{about } 3 \text{ for } M=7, \\ &\text{about } 2 \text{ for } M=6, \\ &\text{about } 1 \text{ for } M=5, \end{aligned}$$

for shallow earthquakes.

Observed amplitude spectrum has a maximum point as mentioned above, and rapidly decreases in the longer period-range from the maximum, while this function does not decrease in the range concerned and has the maximum at zero frequency. Therefore, this function does not exactly represent the observed wave-form. But, since we can approximately estimate the position of the maximum point for any magnitude, it may be possible to derive the spectral structures for respective magnitudes. It is now concluded that P wave in this group changes its wave-form with the magnitude in obedience to such a systematic way as expressed by the above relation. In other words, the first half cycle of P wave becomes long with the magnitude in such a way as stated above.

Both inclinations of amplitude and phase spectra of the deep earthquakes are, as mentioned already, relatively small compared with the shallow shocks of the same order of magnitude. This means that the P wave-form of the deep shock is generally sharper than that of the shallow one. This fact seems very interesting, suggesting the differences in the origin mechanism and in the nature of materials at respective depths.

**(vi) Group B.**

Phase spectra of the earthquakes in group B have large negative inclinations which depend on the magnitude as stated earlier. This systematic difference of the phase spectrum between two groups A and B suggests some essential difference of P wave-forms in the two groups. It will be made clear that it is practically convenient to consider that the large inclination of phase spectrum in this group is brought about by the superposition of a later phase.

Referring to the previous section (iii), if the amplitude ratio  $\alpha$  of a



later phase to the first P wave is larger than unity, the phase spectrum decreases linearly by  $2\pi$  when  $\omega\tau$  increases by  $2\pi$  as shown in Fig. 43(b), where  $\tau$  is the time interval between the P and the later phase concerned. The phase spectrum oscillates around this linear decrease, and this fluctuation becomes larger when the value of  $\alpha$  increases. On the other hand, if  $\alpha$  is slightly larger than unity, the amplitude spectrum has sharp troughs and the phase spectrum shows nearly a linear decrease. These behaviours of both amplitude and phase spectra will be clearly seen in Fig. 43 (b). Many spectra in group B have nearly the same features as to the amplitude and phase as just stated above. This fact means that P waves of group B are characterized by the existence of a later phase with large amplitude. It is interesting to note that, in most earthquakes, the time of incidence of the later phase expected from both spectra coincides with the beginning of the second back swing after the first half cycle of P motion. Actually, P waves in this group generally consist of one and a half cycles of oscillation, and usually the amplitude of the second back swing is larger than the first one. Therefore, it is convenient, at least for the practical treatment, to consider the P wave of this group as a superposition of the first and the next shocks. Thus, the large negative inclination of the phase spectrum and also rather complicated shape of the amplitude spectrum with troughs are considered to be caused by the particular form of P wave in this group.

This thought seems to be supported by examining the results obtained from some earthquakes. In the case of the Mexico earthquake of May 19, 1962, which was already treated in the earlier section, the phase spectra at Alert, Malaga, Ponta Delgada and La Paz have a much smaller decrease than those at other stations, which are nearly the same as in group A. (Fig. 41). The former 4 stations are all situated in the azimuths close to each other, suggesting that two phases in the problem have separated generations at the origin rather than such a particular phase as a whole as directly constructed from the observed amplitude and phase spectra. On the other hand, this azimuthal difference was not observed in some other earthquakes, for example, the Iran earthquake of Sept. 1, 1962 and the Japan earthquake of Apr. 12, 1962 (Section (iii)). If, however, the smaller inclination observed at the four stations in the case of the Mexico earthquake cited above which is not so different from that in group A is the real spectrum of P wave and the larger inclination is the apparent one

caused by the overlapping of a later phase, the observed spectrum does not necessarily agree with the expected one. We can see these circumstances, for instance, in the case of the Banda Sea earthquake in Fig. 30. Two troughs in the amplitude spectrum at about 7.5 and 14 c/m seem to be caused by the second back swing designated by the letter  $x$  in the small figure inserted. If this is the case, referring to the equation (10) in Section (iii), the apparent decrease of phase spectrum should be  $4\pi$  from 0 to 15 c/m. Since the decrease of the observational phase spectrum is about  $4\pi$  from 0 to 15 c/m, the phase spectrum of the "supposed" P wave becomes zero at all frequencies, which does not seem the right result.

Some earthquakes were so far classified in group A because of their small inclinations of phase spectra (Figs. 16, 17, 18 and 19). It is now considered more plausible for these earthquakes to be classified in group B from two points of view. The phase spectra shown in these figures have seriously oscillatory behaviours and their general trend is more curved compared with other earthquakes in group A. These phase spectra concerned are very much like those of the Mexico earthquake of May 19, 1962 above-cited, observed at Alert, Malaga, Ponta Delgada and La Paz. It seems, therefore, natural that the observed wave-forms of these earthquakes in Figs. 16, 17, 18 and 19 are also similar to that of the Mexico earthquake. In these cases, the amplitude ratio,  $\alpha$ , is considered to be slightly smaller than unity. Accordingly, these earthquakes may be more reasonably classified in group B.

Thus, it may be considered more likely that the boundary between groups A and B is not a definite one but that its change is gradual, and some earthquakes are situated at an intermediate position between the two. It is interesting, however, that those intermediate earthquakes are all of shallow focus.

It is now the important problem to make the nature of this "supposed" later phase clear. In Fig. 49, is shown the relation between the magnitude and the time interval,  $\tau$ , which is the duration between the first P motion and the arrival of the later phase inferred from both amplitude and phase spectra. It is clearly seen in this figure that  $\tau$  increases with the magnitude. This systematic behaviour is quite natural, because the time interval  $\tau$  approximately corresponds to the first half period of P wave and it is well known that the half period of P wave increases with the magnitude. But,

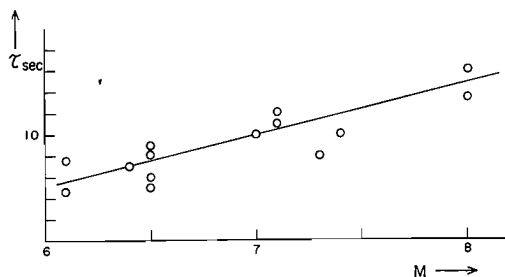


Fig. 49 Relation between the magnitude and the time interval,  $\tau$ .

we can see from this result that the second back swing which is considered as a later phase here is not such an ordinary later phase as pP, PP and others but something related to the origin mechanism. Unfortunately, it is not possible at the present stage to discuss the cause and nature of this second back swing in detail. In order to do such a kind of research, it is necessary to take into consideration some other methods.

The new classification, A' and B', in which some earthquakes are changed from group A into B, is tentatively shown in the column in Table I, headed by the Classification II.

**(vii) Group C'.**

It is seen that there is another kind of group, being inferred from the spectral structure and the observed wave-form. Figs. 26, 31 and 32 are considered to belong to a group of a third kind. P waves of these three earthquakes are characterized by superposition of later phases which are shown by the arrows, with the same direction of movement as the first motion. Both amplitude and phase spectra are explainable by these later phases without any contradiction. Two of these earthquakes are of rather deep focus and therefore the later phases designated by letters  $x$  and  $y$  are not considered the ordinary later phases but something related to the movement at the origin. We shall call them group C' as shown in the column named Classification II in Table I.

**(viii) Distribution of focal depth in each group.**

It was already mentioned in the previous sections that there is a particular depth-range for each group, A' and B', in which the earthquakes in each group prevalingly occur. This nature was made clearer by the new classification, A' and B'.

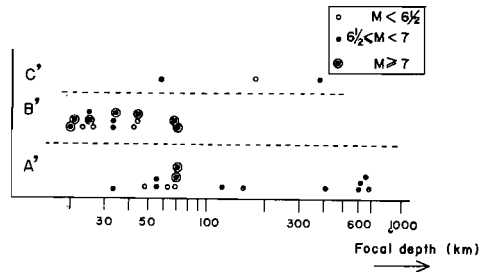


Fig. 50 Distribution of the focal depth in three groups A', B' and C'.

As seen in Fig. 50, the new group A' consists of the earthquakes deeper than, say 40 km and seldom includes very shallow earthquakes which are supposed to have occurred in the crust. On the other hand, most in group B' are shallower than several tens km. Extremely deep earthquakes are not included in this group. It is to be noted that in the depth-range, say 40 to 80 km, occur the earthquakes of both groups, and so this depth-range may be considered as the boundary between two groups. These results are no other than the well known fact that the wave-form of the deep earthquake generally differs from that of the shallow one, but anyway this is an interesting fact suggesting the differences in the earthquake-occurrence mechanism at respective depths.

#### 4. Concluding remarks for Part I.

- (i) P waves of forty earthquakes were Fourier analysed for the purpose of investigating the origin mechanism.
- (ii) The obtained amplitude and phase spectra were examined regarding their changes with the epicentral distance, the azimuth and the location of station. It is concluded, at least as to their general features, that the observed spectra keep fundamentally their characteristics which should be determined by the radiation mechanism at the origin.
- (iii) These earthquakes were classified into two main groups from the standpoint of phase spectrum. In one group named A', the phase spectrum shows relatively small variation with the wave-frequency, while in another group named B', it shows rather large inclination, the value of which changes depending on the magnitude.

- (iv) These phenomena are essentially brought about by the differences in the P wave-form in two groups. Namely, P wave-form in group A' is impulsive, but it is oscillatory for group B'. There is another group besides A' and B' in which P wave-form somewhat differs from the other two groups.
- (v) Distributions of focal depth differ in the two groups, A' and B'. In group A', the depth-range in which most earthquakes occur is deeper than, say 40 km, while in group B', it is shallower than several tens km. Therefore, the mechanism of earthquake-occurrence is expected to change its nature in the depth-range of, say from 40 to 80 km.
- (vi) The amplitude and phase spectra of P wave in group A' are well explained by assuming the function  $t^p e^{-1.2t}$  as the wave-form of incidence, in which the value of p seems a function of magnitude. The P wave of deep earthquakes seems to have sharper wave-form than that of shallow earthquakes. This means that the value of p is small for the deep earthquake.
- (vii) The large variation of phase spectrum with wave-frequency in group B' is considered an apparent phenomenon caused by the existence of the later phase of large amplitude. This phase seems to be related to the radiation mechanism at the origin, because the time interval of arrival times of this phase and P wave always increases with the magnitude.
- (viii) It is important to clarify by what reason these differences in the P wave-form of earthquakes in these three groups, or in other words, of earthquakes occurring at different depths, give rise to, and what relation they have to the mechanism of earthquake-occurrence. By solving these problems, it will be possible even to make clear the aspects of the accumulation and release of earthquake energy at respective depths and regions. In order to solve these problems completely, it may be necessary to allow for various methods of research such as the seismometric investigation and the fault-plane solution method as well as the spectral analysis. In the succeeding article, such problems will be treated with.

### Acknowledgement

The present article is a part of the work done at the Dominion Observatory, Canada, during the writer's stay as a Postdoctorate Fellow of the National Research Council, Canada. The writer wishes to express his hearty thanks to Dr. J. H. Hodgson for his kind advice and encouragement throughout this research. The writer also wishes to thank Prof. J. Oliver of Lamont Geological Observatory, Columbia University; Prof. W. Stauder of Saint Louis University; Prof. H. F. Birkenhauer, S. J. of John Carroll University; Prof. D. H. Shurbet of Texas Technological College; and the Director of the United States Coast and Geodetic Surveys, for their generous permission for the writer to analyse their valuable seismograms.

### References

- Ben-Menahem, A. (1962): Radiation of Seismic Body Waves from a Finite Moving Source in the Earth, *Journ. Geophys. Res.*, 67, 345.
- Blackman, R. B. and Tukey, J. W. (1958): *The Measurement of Power Spectra*, Publ., Dover.
- Hodgson, J. H. (Editor) (1957): *The Mechanics of Faulting, With Special Reference to the Fault-plane Work*, Publ. Dom. Obs., Ottawa, 24, 251.
- Hodgson, J. H. (Editor) (1960): *A Symposium on Earthquake Mechanism*, Publ. Dom. Obs., Ottawa, 24, 299.
- Honda, H. (1962): *Earthquake Mechanism and Seismic Waves*, Geophys. Notes, Tokyo Univ., 15 (Suppl.), 1.
- Kasahara, K. (1957): *The Nature of Seismic Origin as Inferred from Seismological and Geodetic Observations*, Bull. Earthq. Res. Inst., 35, 473.
- Kasahara, K., (1960): *An Attempt to Detect Azimuth Effect on Spectral Structures of Seismic Waves. (The Alaskan Earthquake of April 7, 1958)*, Bull. Earthq. Res. Inst., 38, 207.

## Publications of the Disaster Prevention Research

### Institute

The Disaster Prevention Research Institute publishes reports of the research results in the form of bulletins. Publications not out of print may be obtained free of charge upon request to the Director, Disaster Prevention Research Institute, Kyoto University, Kyoto, Japan.

### Bulletins :

- No. 1 On the Propagation of Flood Waves by Shoitiro Hayami, 1951.
- No. 2 On the Effect of Sand Storm in Controlling the Mouth of the Kiku River by Tojiro Ishihara and Yuichi Iwagaki, 1952.
- No. 3 Observation of Tidal Strain of the Earth (Part I) by Kenzo Sassa, Izuo Ozawa and Soji Yoshikawa. And Observation of Tidal Strain of the Earth by the Extensometer (Part II) by Izuo Ozawa, 1952.
- No. 4 Earthquake Damages and Elastic Properties of the Ground by Ryo Tanabashi and Hatsuo Ishizaki, 1953.
- No. 5 Some Studies on Beach Erosions by Shoitiro Hayami, Tojiro Ishihara and Yuichi Iwagaki, 1953.
- No. 6 Study on Some Phenomena Forcelling the Occurrence of Destructive Earthquakes by Eiichi Nishimura, 1953.
- No. 7 Vibration Problems of Skyscraper. Destructive Element of Seismic Waves for Structures by Ryo Tanabashi, Takuzi Kobori and Kiyoshi Kaneta, 1954.
- No. 8 Studies on the Failure and the Settlement of Foundations by Sakurō Murayama, 1954.
- No. 9 Experimental Studies on Meteorological Tsunamis Traveling up the Rivers and Canals in Osaka City by Shoitiro Hayami, Katsumasa Yano, Shohei Adachi and Hideaki Kunishi, 1955.
- No.10 Fundamental Studies on the Runoff Analysis by Characteristics by Yuichi Iwagaki, 1955.
- No.11 Fundamental Considerations on the Earthquake Resistant Properties of the Earth Dam by Motohiro Hatanaka, 1955.
- No.12 The Effect of the Moisture Content on the Strength of an Alluvial Clay by Sakurō Murayama, Kōichi Akai and Tōru Shibata, 1955.
- No.13 On Phenomena Forerunning Earthquakes by Kenzo Sassa and Eiichi Nishimura, 1956.
- No.14 A Theoretical Study on Differential Settlements of Structures by Yoshitsura Yokoo and Kunio Yamagata, 1956.
- No.15 Study on Elastic Strain of the Ground in Earth Tides by Izuo Ozawa, 1957.
- No.16 Consideration on the Mechanism of Structural Cracking of Reinforced Concrete Buildings Due to Concrete Shrinkage by Yoshitsura Yokoo and S. Tsunoda, 1957.
- No.17 On the Stress Analysis and the Stability Computation of Earth Embankments by Kōichi Akai, 1957.
- No.18 On the Numerical Solutions of Harmonic, Biharmonic and Similar Equations by the Difference Method Not through Successive Approximations by Hatsuo Ishizaki, 1957.

- No.19 On the Application of the Unit Hydrograph Method to Runoff Analysis for Rivers in Japan by Tojiro Ishihara and Akiharu Kanamaru, 1958.
- No.20 Analysis of Statically Indeterminate Structures in the Ultimate State by Ryo Tanabashi, 1958.
- No.21 The Propagation of Waves near Explosion and Fracture of Rock (I) by Soji Yoshikawa, 1958.
- No.22 On the Second Volcanic Micro-Tremor at the Volcano Aso by Michiyasu Shima, 1958.
- No.23 On the Observation of the Crustal Deformation and Meteorological Effect on It at Ide Observatory and On the Crustal Deformation Due to Full Water and Accumulating Sand in the Sabo-Dam by Michio Takada, 1958.
- No.24 On the Character of Seepage Water and Their Effect on the Stability of Earth Embankments by Kōichi Akai, 1958.
- No.25 On the Thermoclasticity in the Semi-infinite Elastic Solid by Michiyasu Shima, 1958.
- No.26 On the Rheological Characters of Clay (Part 1) by Sakurō Murayama and Tōru Shibata, 1958.
- No.27 On the Observing Instruments and Tele-metrical Devices of Extensometers and Tiltmeters at Ide Observatory and On the Crustal Strain Accompanied by a Great Earthquake by Michio Takada, 1959.
- No.28 On the Sensitivity of Clay by Shinichi Yamaguchi, 1959.
- No.29 An Analysis of the Stable Cross Section of a Stream Channel by Yuichi Iwagaki and Yoshito Tsuchiya, 1959.
- No.30 Variations of Wind Pressure against Structures in the Event of Typhoons by Hatsuo Ishizaki, 1959.
- No.31 On the Possibility of the Metallic Transition of MgO Crystal at the Boundary of the Earth's Core by Tatsuhiko Wada, 1960.
- No.32 Variation of the Elastic Wave Velocities of Rocks in the Process of Deformation and Fracture under High Pressure by Shogo Matsushima, 1960.
- No.33 Basic Studies on Hydraulic Performances of Overflow Spillways and Diversion Weirs by Tojiro Ishihara, Yoshiaki Iwasa and Kazune Ihda, 1960.
- No.34 Volcanic Micro-tremors at the Volcano Aso by Michiyasu Shima, 1960.
- No.35 On the Safety of Structures Against Earthquakes by Ryo Tanabashi, 1960.
- No.36 On the Flow and Fracture of Igneous Rocks and On the Deformation and Fracture of Granite under High Confining Pressure by Shogo Matsushima, 1960
- No.37 On the physical properties within the B-layer deduced from olivine-model and on the possibility of polymorphic transition from olivine to spinel at the 20° Discontinuity by Tatsuhiko Wada, 1960.
- No.38 On Origins of the Region C and the Core of the Earth —Ionic-Intermetallic-Metallic Transition Hypothesis— by Tatsuhiko Wada, 1960.
- No.39 Crustal Structure in Wakayama District as Deduced from Local and Near Earthquake Observations by Takeshi Mikumo, 1960.
- No.40 Earthquake Resistance of Traditional Japanese Wooden Structures by Ryo Tanabashi, 1960.
- No.41 Analysis With an Application to Aseismic Design of Bridge Piers by Hisao Goto and Kiyoshi Kaneta, 1960.
- No.42 Tilting Motion of the Ground as Related to the Volcanic Activity of Mt. Aso and Micro-Process of the Tilting Motion of Ground and Structure by Yoshiro Itō 1961.
- No.43 On the Strength Distribution of the Earth's Crust and the Upper Mantle, and



- the Distribution of the Great Earthquakes with Depth by Shogo Matsushima, 1961
- No.44 Observational Study on Microseisms (Part 1) by Kennosuke Okano, 1961.
- No.45 On the Diffraction of Elastic Plane Pulses by the Crack of a Half Plane by Michiyasu Shima, 1961.
- No.46 On the Observations of the Earth Tide by Means of Extensometers in Horizontal Components by Izuo Ozawa, 1961.
- No.47 Observational Study on Microseisms (Part 2) by Kennosuke Okano, 1961.
- No.48 On the Crustal Movement Accompanying with the Recent Activity on the Volcano Sakurajima (Part 1) by Keizo Yoshikawa, 1961.
- No.49 The Ground Motion Near Explosion by Soji Yoshikawa, 1961.
- No.50 On the Crustal Movement Accompanying with the Recent Activity of the Volcano Sakurajima (Part 2) by Keizo Yoshikawa, 1961.
- No.51 Study on Geomagnetic Variation of Telluric Origin Part 1 by Junichiro Miyakoshi, 1962.
- No.52 Considerations on the Vibrational Behaviors of Earth Dams by Hatsuo Ishizaki and Naotaka Hatakeyama, 1962.
- No.53 Some Problems on Time Change of Gravity (Parts 1 and 2) by Ichiro Nakagawa, 1962.
- No.54 Nature of the Volcanic Micro-Tremors at the Volcano Aso, Part 1. Observation of a New Type of Long-Period Micro-Tremors by Long-Period Seismograph by Kosuke Kamo, 1962.
- No.55 Nature of the Volcanic Micro-Tremors at the Volcano Aso, Part 2. Some Natures of the Volcanic Micro-Tremors of the 1st kind at the Volcano Aso by Kosuke Kamo, 1962.
- No.56 Nonlinear Torsional Vibration of Structures due to an Earthquake by Ryo Tanabashi, Takuji Kobori and Kiyoshi Kaneta, 1962.
- No.57 Some Problems on Time Change of Gravity (Parts 3, 4 and 5) by Ichiro Nakagawa, 1962.
- No.58 A Rotational Strain Seismometer by Hikaru Watanabe, 1962.
- No.59 Hydraulic Model Experiment Involving Tidal Motion (Parts 1, 2, 3 and 4) by Haruo Higuchi, 1963.
- No.60 The Effect of Surface Temperature on the Crustal Deformations by Shokichi Nakano, 1963.
- No.61 An Experimental Study on the Generation and Growth of Wind Waves by Hideaki Kunishi, 1963.
- No.62 The Crustal Deformations due to the Source of Crack Type (1) by Shokichi Nakano, 1963.
- No.63 Basic Studies on the Criterion for Scour Resulting from Flows Downstream of an Outlet by Yoshito Tsuchiya, 1963.
- No.64 On the Diffraction of Elastic Plane Pulses by a Crack of a Half Plane. (Three Dimensional Problem) by Michiyasu Shima, 1963.
- No.65 A Study on Runoff Pattern and its Characteristics by Tojiro Ishihara and Takuma Takasao, 1963.
- No. 66. Application of Extreme Value Distribution in Hydrologic Frequency Analysis by Mutsumi Kadoya. 1964.
- No. 67 Investigation on the Origin Mechanism of Earthquakes by the Fourier Analysis of Seismic Bodys Waves (I), by Yoshimichi Kishimoto, 1964.

Bulletin No. 67

Published March, 1964

昭和 39 年 3 月 20 日 印 刷

昭和 39 年 3 月 25 日 発 行

編 集 兼 者 京 都 大 学 防 災 研 究 所  
發 行 者

印 刷 者 小 林 積 造

大阪市福島区亀甲町2の62

印 刷 所 日 本 印 刷 出 版 株 式 会 社